

PSEUDOBU LGES IN THE DISK GALAXIES NGC 7690 AND NGC 4593^{1,2}

JOHN KORMENDY^{3,4}, MARK E. CORNELL³, DAVID L. BLOCK⁴, JOHAN H. KNAPEN⁵, EMMA L. ALLARD⁵

Draft version June 12, 2018

ABSTRACT

We present K_s -band surface photometry of NGC 7690 (Hubble type Sab) and NGC 4593 (SBb). We find that, in both galaxies, a major part of the “bulge” is as flat as the disk and has approximately the same color as the inner disk. In other words, the “bulges” of these galaxies have disk-like properties. We conclude that these are examples of “pseudobulges” – that is, products of secular dynamical evolution. Nonaxisymmetries such as bars and oval disks transport disk gas toward the center. There, star formation builds dense stellar components that look like – and often are mistaken for – merger-built bulges but that were constructed slowly out of disk material. These pseudobulges can most easily be recognized when, as in the present galaxies, they retain disk-like properties. NGC 7690 and NGC 4593 therefore contribute to the growing evidence that secular processes help to shape galaxies.

NGC 4593 contains a nuclear ring of dust that is morphologically similar to nuclear rings of star formation that are seen in many barred and oval galaxies. The nuclear dust ring is connected to nearly radial dust lanes in the galaxy’s bar. Such dust lanes are a signature of gas inflow. We suggest that gas is currently accumulating in the dust ring and hypothesize that the gas ring will starburst in the future. The observations of NGC 4593 therefore suggest that major starburst events that contribute to pseudobulge growth can be episodic.

Subject headings: galaxies: evolution — galaxies: individual (NGC 4593, NGC 7690) — galaxies: photometry — galaxies: spiral — galaxies: structure

1. INTRODUCTION

Internal secular evolution of galaxies is the dynamical redistribution of energy and angular momentum that causes galaxies to evolve slowly between rapid (collapse-timescale) transformation events that are caused by galaxy mergers. Driving agents include nonaxisymmetries in the gravitational potential such as bars, oval disks, and global spiral structure. Kormendy (1993) and Kormendy & Kennicutt (2004, hereafter KK) review the growing evidence that secular processes have shaped the structure of many galaxies.

The fundamental way that self-gravitating disks evolve – provided that there is an efficient driving agent – is by spreading (Lynden-Bell & Kalnajs 1972; Lynden-Bell & Pringle 1974; Tremaine 1989; see Kormendy & Fisher 2005 for a review in the present context). In general, it is energetically favorable to shrink the inner parts by expanding the outer parts. In barred galaxies, one well known consequence is the production of “inner rings” around the end of the bar and “outer rings” at about 2.2 bar radii. The most general consequence of secular evolution, and the one that is of interest in this paper, is that some disk gas is

driven to small radii where it reaches high densities, feeds starbursts, and builds “pseudobulges”. Because of their high stellar densities and steep density gradients, pseudobulges superficially resemble – and often are mistaken for – bulges. Following Sandage (1961) and Sandage & Bedke (1994), Renzini (1999) adopts this definition of a bulge: “It appears legitimate to look at bulges as ellipticals that happen to have a prominent disk around them [and] ellipticals as bulges that for some reason have missed the opportunity to acquire or maintain a prominent disk.” We adopt the same definition. Our paradigm of galaxy formation then is that bulges and ellipticals both formed via galaxy mergers (e.g., Toomre 1977; Steinmetz & Navarro 2002, 2003), a conclusion that is well supported by observations (see Schweizer 1990 for a review). Pseudobulges are therefore fundamentally different from bulges – they were built slowly out of the disk. Two well developed examples, one in the unbarred galaxy NGC 7690 and one in the barred galaxy NGC 4593, are the subjects of this paper.

Hierarchical clustering and galaxy merging are well known. Secular evolution is less studied and less well known. We are therefore still in the “proof of concept” phase in which it is useful to illustrate clearcut examples of the results of secular evolution. This paper continues a series (see the above reviews and Kormendy & Cornell 2004) in which we illustrate the variety of disk-like features that define pseudobulges.

2. OBSERVATIONS AND DATA REDUCTIONS

2.1. AAT Infrared Imaging and Data Reduction

NGC 7690 and NGC 4593 show dust absorption features near their centers. Also, if star formation were in progress, there would be a danger that the brightness distributions at visible wavelengths would be affected by strong variations in mass-to-light ratios. We therefore base our results on near-infrared photometry, and we check later that they are not greatly affected by stellar population gradients or by dust absorption.

¹ Based on observations made with the Anglo-Australian Telescope.

² Based in part on observations made with the NASA/ESA Hubble Space Telescope, obtained from the Data Archive at the Space Telescope Science Institute (STScI). STScI is operated by the Association of Universities for Research in Astronomy, Inc., under NASA contract NAS5–26555. The observations of NGC 7690 are associated with program IDs 7331 (NICMOS – Massimo Stiavelli) and 6359 (WFPC2 – Massimo Stiavelli). The observations of NGC 4593 are associated with program IDs 7330 (NICMOS – John Mulchaey), and 5479 (WFPC2 – Matthew Malkan).

³ Department of Astronomy, University of Texas, 1 University Station, Austin, Texas 78712-0259; kormendy@astro.as.utexas.edu, cornell@astro.as.utexas.edu

⁴ Cosmic Dust Laboratory, School of Computational and Applied Mathematics, University of the Witwatersrand, Private Bag 3, WITS 2050, Johannesburg, South Africa; block@cam.wits.ac.za

⁵ Centre for Astrophysics Research, University of Hertfordshire, Hatfield, Herts AL10 9AB, United Kingdom; j.knapen@star.herts.ac.uk, allard@star.herts.ac.uk

Near-infrared images of both galaxies were obtained with the InfraRed Imaging Spectrograph 2 (IRIS2; Tinney et al. 2004) at the $f/8$ Cassegrain focus of the Anglo-Australian Telescope (AAT). We used IRIS2 in its wide-field imaging mode; this provides a field of view of 7.7×7.7 sampled at a scale of $0''.4486 \text{ pixel}^{-1}$. The bandpass was K_s for both galaxies. We imaged NGC 7690 for a total on-source exposure time of 56 m. These observations were taken on 2004 July 1. For NGC 4593, we obtained 52 m of on-source exposure piecemeal during the nights of 2004 June 30, July 1, July 2, and July 4. Individual images from different nights were combined during the reduction process.

Our observing techniques were similar to those described in Knapen et al. (2003) and in Block et al. (2004). Individual 8 s exposures were co-added into raw images of 56 s exposure time. In contrast to our earlier work and taking advantage of the large IRIS2 field of view compared to the size of the galaxies, we did not alternate telescope pointings between the target and a nearby, blank background field. Instead, we used a grid of four pointings, each of which imaged the galaxy in one quadrant of the detector array. This ‘‘quadrant-jitter’’ method has the advantage of high observing efficiency, because no separate background exposures are needed, but the disadvantage that the galaxy image must be removed from the raw exposures when constructing background sky images.

The AAT K_s -band images were reduced in IRAF (Tody 1986) using our own procedures. The NGC 7690 data reductions were relatively simple, because the images were obtained at low airmass on a single photometric night. The galaxy was observed in quadrant-jitter mode, so it was centered in a different quadrant of the detector in each frame of a consecutive series. We constructed a flat-field frame for each detector quadrant from the median of all images with no galaxy in that quadrant. The images were adjusted for any additive offset before computing the median. The NGC 7690 field had few stars, and none remained in the final flat field. Once the quadrants were flattened, the galaxy quadrants were registered and stacked using a median combine, again correcting for additive offsets. The final stacked frame was quite flat, so a single constant sky value was subtracted. In contrast, the NGC 4593 images were taken over 4 nights, at high airmass, and in more variable conditions. The background shape varied enough so that the simple assumptions used for NGC 7690 did not work for NGC 4593. We constructed a flat-field frame from all of the NGC 4593 images as before. After flat-fielding, we subtracted from each galaxy frame a sky frame constructed from the median of the 4 frames taken nearest in time to the galaxy frame but with the galaxy in a different quadrant. Stars in the field were masked before constructing the flat-field and sky frames.

The reduced NGC 7690 image has PSF FWHM = $1''.0$ and the NGC 4593 image has FWHM = $1''.6$.

2.2. Additional Archival Images

The images used for surface photometry were archival *Hubble Space Telescope* (HST) WFPC2 F606W images, HST NICMOS F160W images, archival 2MASS images (extended source catalog tile for NGC 7690 and a Large Galaxy Atlas image for NGC 4593), and the AAT K_s -band images obtained with IRIS2. To improve signal-to-noise, the 2MASS J , H , and K_s images were added together. The background was removed from the NGC 7690 2MASS tile by masking the stars and then fitting and subtracting a quadratic surface. The background in the 2MASS image of NGC 4593 was already sufficiently flat.

Cosmic ray hits and bad pixels in the NICMOS data were removed using the `tvzap` command in Jon Holtzman’s (<http://astronomy.nmsu.edu/holtz/xvista>) implementation of VISTA (Lauer et al. 1983; Stover 1988). This replaces user-selected pixels with the median of the surrounding 5×5 pixels. Cosmic ray hits in the WFPC2 image of NGC 7690 were removed using the STSDAS task `CRREJ`. The central, bad 1 – 2 columns in the NICMOS data were fixed by linearly interpolating the neighboring pixel values line by line. Gaps in the mosaiced Wide Field Camera image were also filled via linear interpolation. The HST PC V-band image of NGC 4593 that is used in Figure 3 was cleaned of cosmic rays using the IRAF script `L.A.COSMIC` (van Dokkum 2001) and `VISTA tvzap`.

Finally, any remaining sky background level was computed as the average of the modes of the pixel values in several sky boxes chosen to be free of galaxy light or interfering objects. The galaxies fill the HST Planetary Camera (PC) and NICMOS fields of view. For the PC, the sky flux was measured on the Wide Field Camera images and scaled to the PC pixels. For the NICMOS image, the sky was taken as zero for NGC 7690. For NGC 4593, the sky value for the NICMOS image was chosen to optimize the agreement between the major-axis cuts as measured on the NICMOS and AAT images in the radius range $3'' \leq r \leq 13''$.

2.3. Surface Photometry

Before fitting ellipses and calculating profile cuts, interfering foreground and background objects were identified using Source Extractor (Bertin & Arnouts 1996) and masked. Any remaining stars were identified visually and masked as well.

Position angle and ellipticity profiles as a function of major-axis radius r were derived from ellipse fits using the method of Bender & Möllenhoff (1987) and Bender et al. (1988) as implemented in MIDAS (Banse et al. 1988) by Bender and by Saglia (2003, private communication). Position angles are measured east of north. Some profiles were extended using ellipse fits made by GASP (Cawson 1983; Davis et al. 1985), which is slightly more robust at low S/N or when isophotes are incomplete at the edge of the field of view.

Surface brightness cuts along the major axis, the minor axis, and (for NGC 4593) the bar were produced using a program that averages pixel values in a 25° -wide, pie-shaped wedge. Therefore, more pixels are included at large radii where the S/N is low. Masked pixels are left out of the average. The cuts on opposite sides of the galaxy center were averaged.

The various cut profiles were shifted in mag arcsec^{-2} to match up as well as possible. The K_s -band zeropoint for NGC 7690 was derived from 2MASS, $5''$ - and $7''$ -radius, circular-aperture photometry applied to the HST NICMOS F160W (H -band) image. The K_s -band zeropoint for NGC 4593 was transferred from 2MASS by measuring the galaxy magnitude in the Large Galaxy Atlas image (Jarrett et al. 2003) and in our AAT image within the largest (radius = $95''$) aperture that fits within our image. For NGC 7690, the V -band zeropoint was derived from aperture photometry by Wegner (1979). For NGC 4593, the WFPC2 image is saturated, making calibration via aperture photometry problematic. Instead we used the transformation from F606W to Johnson V given by Holtzman et al. (1995), assuming that $V - I = 1.25$ from the aperture photometry by McAlary et al. (1983) as tabulated by Prugniel & Héraudeau (1998).

The cut profiles were smoothed by averaging values in bins

of width 0.04 in $\log r$. Profiles were truncated where they were affected by seeing at small radii and low S/N at large radii.

The $V - K_s$ cut profile was created from calibrated V and K_s composite profiles. The V composite profile was created from a cut from the Planetary Camera image inside a radius of $20''$, and the cut from the Wide Field Camera beyond that. Similarly, the K_s composite profile was created from the NICMOS profile inside $10''$ and the AAT profile outside that.

The $V - K_s$ images were created by taking the ratio of the sky-subtracted WFPC2 F606W V and AAT K_s frames, after convolving the WFPC2 frames with gaussians to match the AAT PSFs. Figures 1 and 3 shows the logarithms of the ratio images.

3. NGC 7690

NGC 7690 is an unbarred, Sab galaxy illustrated in the Carnegie Atlas (Sandage & Bedke 1994). In Tully (1988) group 61 $-0 +16$; its group's mean recession velocity of $1495 \pm 59 \text{ km s}^{-1}$ together with a Hubble constant of $71 \text{ km s}^{-1} \text{ Mpc}^{-1}$ (Spergel et al. 2003) imply a distance of 21 Mpc. For a Galactic absorption of $A_B \simeq 0.045$ (Schlegel et al. 1998) and a total B -band apparent magnitude of $B_T = 13.0$ (de Vaucouleurs et al. 1991: RC3), the absolute magnitude is $M_B = -18.7$. NGC 7690 is therefore a reasonably normal, low-luminosity disk galaxy. Its relatively early Hubble type implies that it should have a substantial bulge (e. g., Simien & de Vaucouleurs 1986). In particular, NGC 7690 is earlier in Hubble type than the relatively sharp transition observed to occur at Sb/Sbc between early-type galaxies that mostly contain classical bulges and late-type galaxies that mostly contain pseudobulges (see KK for a review). NGC 7690 nevertheless proves to contain a well developed pseudobulge.

The pseudobulge of NGC 7690 was discovered by Carollo et al. (1998); their V -band image is included in Figure 13 of KK. An *HST* F160W image from Carollo et al. (2002) is shown in the upper-right panel of our Figure 1. Qualitatively, the center of NGC 7690 looks disk-like, so much so that in the ‘‘Bulge?’’ column of Table 2 in Carollo et al. (1998), they do not even list NGC 7690 as having an ‘‘IB’’ = ‘‘irregular bulge’’, which is essentially equivalent to what we call a pseudobulge. Instead, the entry is ‘‘No?’’. NGC 7690 was chosen for this paper because we wanted to investigate the (pseudo)bulge quantitatively with near-infrared surface photometry.

The results are shown in Figure 1. The blue and red $\mu(r)$ points are major- and minor-axis brightness cuts calculated as discussed in § 2.3. Excellent agreement between the AAT and 2MASS profiles provides an important check of our reduction procedures. The $\epsilon(r)$ and $PA(r)$ points are isophote ellipticity and position angle profiles calculated by fitting elliptical isophotes to the images identified in the key. Calculations of the $V - K_s$ color profile (top-left plot) and image (lower-right) are discussed in § 2.3. The profiles are plotted against $\log r$ to illustrate the behavior at small and large radii and also against linear radius r so that an exponential outer disk – and departures of the inner profile above it – can easily be recognized.

Fig. 1 shows three quantitative signatures of a pseudobulge:

First, the central component illustrated by Carollo and collaborators forms a clear shelf in the brightness distribution at major- and minor-axis radii of $6''$ and $3''$, respectively. That is, it has the morphology of a lens (Freeman 1975; Kormendy 1979, 1981; Buta & Combes 1996), not a bar. A bar would form a shelf in the major-axis profile only. In

contrast, a lens⁶ is defined as a shelf of nearly constant surface brightness seen along both the major and minor axes. Lenses have intrinsic axial ratios $\sim 0.9 \pm 0.05$ in the equatorial plane (see the above papers), whereas bars in early-type galaxies have axial ratios of ~ 0.1 to 0.3 in the equatorial plane (see Sellwood & Wilkinson 1993 for a review). In other words, the shape distributions of lenses and bars do not overlap. Lenses and bars are physically different. In fact, barred galaxies often contain both components, with the bar filling the lens in one dimension (see the above papers). However, unbarred galaxies can also have strong lenses (e. g., NGC 1553: Freeman 1975; Kormendy 1984). Note further that lenses and ‘‘inner rings’’ (bright rings that generally encircle the end of the bar) are also different (e. g., Sellwood & Wilkinson 1993; Buta & Combes 1996): inner rings are relatively dark inside. Also, rings are narrow in the radial direction and therefore must have small radial velocity dispersions, whereas lenses are observed to have large radial velocity dispersions (e. g., Kormendy 1984). The main bars in early-type galactic disks have radii of ~ 1.4 exponential scale lengths (Erwin 2005), and – as noted above – the radii of lenses and inner rings are closely similar to the sizes of their associated bars. Distinctly smaller versions of all of these phenomena – nuclear bars, nuclear lenses (often but not always associated with nuclear bars), and nuclear rings – also occur, usually but not always in galaxies that also contain larger, ‘‘main’’ bars or ovals. We belabor these points because lenses are less well known in the astronomical community than bars or inner rings. The $6'' \times 3''$ shelf in the brightness distribution of NGC 7690 is a nuclear lens without an associated nuclear or main bar.

The nuclear lens is 1.5 to $2 K_s \text{ mag arcsec}^{-2}$ higher in surface brightness than the inward extrapolation of the outer disk's almost-exponential brightness profile. It therefore forms part of what would conventionally be identified as the bulge. We would like to classify a bulge as the E-like part of a galaxy. In practice, this is not straightforward for non-edge-on galaxies. Therefore, Carollo et al. (1999) adopt the surrogate definition that a bulge is the central part of the galaxy that is brighter than the inward extrapolation of the outer disk's exponential brightness profile. By this definition, the nuclear lens in NGC 7690 is part of the galaxy's bulge. But bulges and elliptical galaxies generally have simple brightness profiles consisting of a single Sérsic (1968) $\log I \propto r^{1/n}$ profile (possibly with a cuspy core) and not a shelf in the brightness profile such as the one in NGC 7690.

The second pseudobulge indicator is that the nuclear lens – the shelf in the inner brightness profile – is clearly a disk. This was already evident from the images in Carollo et al. (1998, 2002), as shown here in Figure 1. The nuclear disk in the top-right panel has the same apparent flattening and position angle as the outer disk shown in the middle image panel. We see this result quantitatively in the ϵ and PA plots. The $r = 6''$ shelf in the brightness profile has precisely the same ellipticity and PA as the disk farther out. It is not plausible that this is due to internal absorption, because the V -band ellipticities and position angles (crosses in Figure 1) agree with the K_s -band ones at all radii that are relevant to our conclusions. Since the K_s -band extinction is about one-tenth as big as the V -band

⁶ Lens components should not be confused with lenticular galaxies, i. e., with the name for S0 galaxies (Sandage 1961) that is adopted by de Vaucouleurs and collaborators (e. g., RC3). Many S0 galaxies do not contain lenses, and many Sa and later-type galaxies do contain lenses. This confusion is unfortunate, but it is thoroughly embedded in the literature.

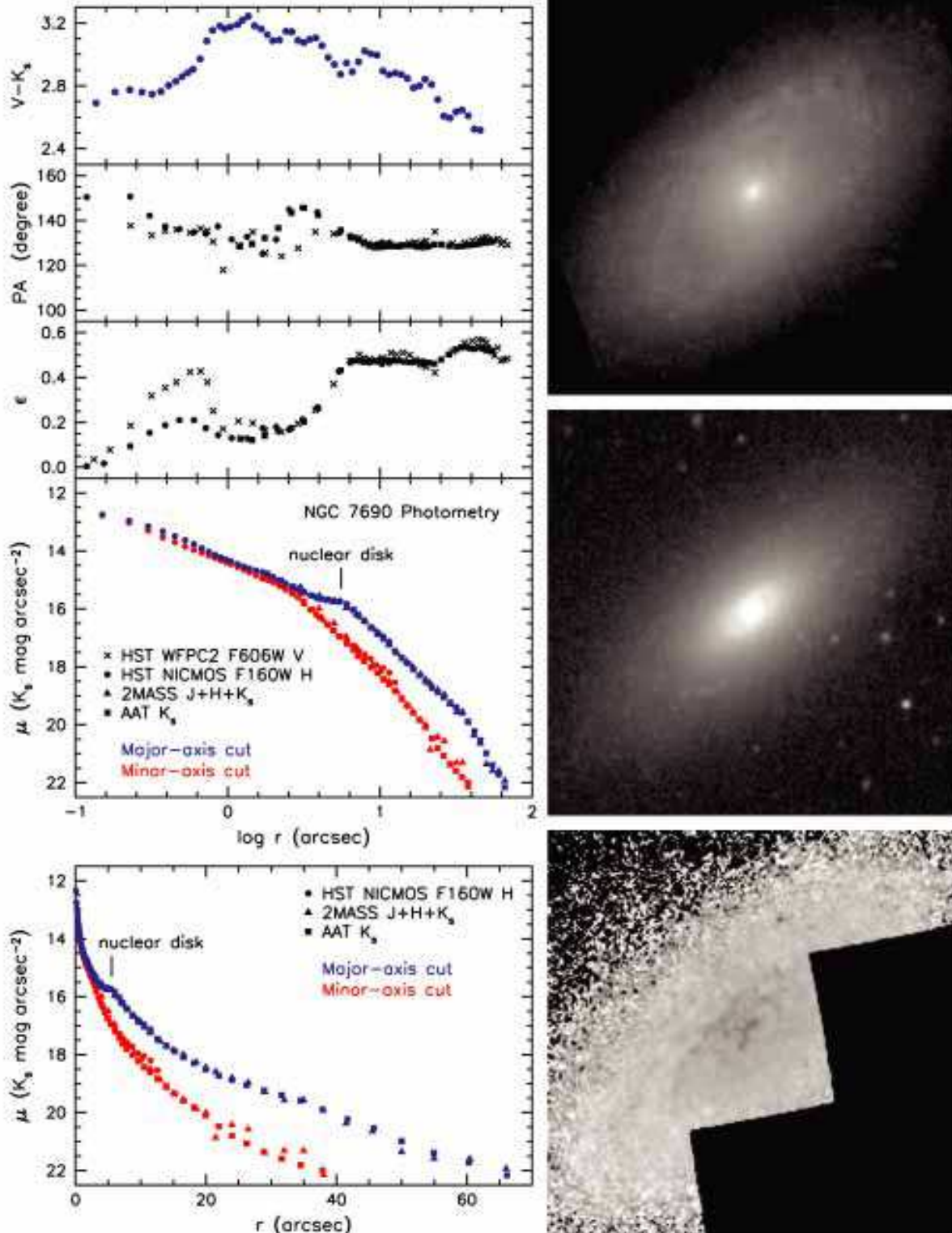


FIG. 1.— NGC 7690 pseudobulge – top image: $18'' \times 18''$ *HST* NICMOS F160W image from Carollo et al. (2002); middle: $91'' \times 91''$ AAT K_s -band image discussed in §2; the images are shown at different logarithmic intensity stretches. Bottom: $V-K_s$ color image constructed from the above K_s frame and from a V -band (F606W) image taken with *HST* by Carollo et al. (1998; they also show an unsharp-masked image). The intensity stretch is linear in mag arcsec^{-2} ; white corresponds to $V-K_s = 0.8$, and black corresponds to $V-K_s = 3.5$. The middle and bottom panels show the same field of view. North is up and east is at left in all images. A large-scale ($9'' \times 9''$) $V-H$ color image obtained with *HST* is illustrated in Carollo et al. (2002). The left panels above show surface photometry as a function of log radius (top) and linear radius (bottom). Brightness and $V-K_s$ profiles are 25° -wide cuts along the major axis ($PA = 129^\circ$) and minor axis ($PA = 39^\circ$) color-coded as indicated in the key and with opposite sides of the galaxy averaged. Isophote ellipticities ϵ and major-axis position angles PA are derived from isophote fits to the images indicated in the key.

extinction (e. g., Cox 2000), this implies that extinction does not significantly affect the parameters at either wavelength,

unless unrealistically gray extinction is postulated. From $r \simeq 6''$ outward, the ellipticity and PA change very little, consistent with a nearly circular main disk at nearly constant inclination. We conclude that the nuclear lens, i. e., the outer part of what would conventionally be identified as the bulge of NGC 7690, is as flat as the galaxy’s disk. This is the most clearcut signature of a pseudobulge in NGC 7690 (see KK for pseudobulge classification criteria).

The surface brightness of the nuclear disk is nearly constant interior to its sharp outer edge. Not surprisingly, the ellipticity drops rapidly inward as the profile of this highly-inclined galaxy becomes dominated by a less flattened center. This feature may be but is not necessarily a classical bulge. It would be no surprise if the pseudobulge part of NGC 7690 were embedded in a classical bulge, because secular evolution can build a pseudobulge inside a pre-existing bulge (see KK). But several arguments suggest that a classical bulge is not the main feature near the center. First, the PA profile shows a clear twist centered at $r \simeq 3''$. The ellipticity starts to drop suddenly toward the center at the radius $r \simeq 6''$ where the twist starts, and it continues to drop throughout the radius range of the twist. This combination is a characteristic of a weak bar or weak spiral arms. Bars and spiral arms are disk features. Thus, even interior to its sharp outer edge, the signs are that the galaxy is dominated by a disk.

The third pseudobulge indicator is the lack of a steep color gradient between a bluish disk and a red and much older bulge. The $V - K_s$ color image (bottom-right in Figure 1) and profile both show that, apart from a few irregular dust features that are easily masked out in the photometry, there is no significant color difference between the inner part of the outer disk and the nuclear disk. Indeed, the $V - K_s$ profile is completely continuous from the disk-dominated outer galaxy to the bulge-dominated inner galaxy. This is an example of a general phenomenon: (pseudo)bulge and disk colors correlate (Peletier & Balcells 1996; Gadotti & dos Anjos 2001). Bulges and disks both show large ranges in colors, but “bulges are more like their disk[s] than they are like each other” (Wyse et al. 1997). Courteau et al. (1996) and Courteau (1996) interpret such correlations as products of secular dynamical evolution. As noted above, there is no sign in NGC 7690 of a discontinuity in stellar population between an old, non-star-forming bulge and a younger disk, as one would expect for a classical bulge (Sandage & Bedke 1994).

Note that the small color gradient from outer disk to nuclear lens implies, since K_s extinctions are so much smaller than V extinctions, that the shelf in the brightness profile is a real feature in the stellar density and not an artifact of absorption.

Several classification criteria agree, so it seems safe to conclude that NGC 7690 contains a pseudobulge. This may or may not coexist with a small classical bulge – we cannot be certain from the data at hand, although no observation points compellingly to a classical bulge component.

We conclude that NGC 7690 is an example of secular evolution in action. This is particularly interesting because the Sab galaxy NGC 7690 is earlier in type than the galaxies⁷ that most commonly contain pseudobulges. Also, there is no obvious engine for secular evolution, such as a bar, oval distortion, or global spiral structure. NGC 7690 therefore contributes to the accumulating evidence that secular evolution occurs in a wide variety of galaxies.

⁷ We note, however, that even S0s can contain pseudobulges (KK).

4. NGC 4593

NGC 4593 is a structurally normal SBb galaxy (Sandage 1961; Sandage & Bedke 1994). We adopt a distance of 35 Mpc (Tully 1988 group 11 –29), then $B_T = 11.67$ (RC3) implies that $M_B = -21.2$. NGC 4593 is therefore a high-luminosity disk galaxy. Moreover, it has a well developed engine for secular evolution in the form of a high-amplitude bar. Secular evolution is likely to be rapid. Our photometry of NGC 4593 proves to be consistent with this expectation (Figure 2).

4.1. Near-Infrared Photometry: Evidence for a Pseudobulge

NGC 4593 is a well known Seyfert I galaxy (Lewis et al. 1978; MacAlpine et al. 1979). The nuclear point source is very bright (*HST* F606W mag ~ 17.1 at $r \leq 0''.09$); it completely swamps the central brightness distribution of the galaxy (MRK 1330 in Figure 1 of Malkan et al. 1998). Since this is not star light, it is important that we subtract it in our analysis of the brightness distribution. We did this for the *HST* NICMOS image by subtracting a PSF calculated with *Tiny Tim* (Krist & Hook 2004) and scaled in total intensity to remove the diffraction spikes and other small-scale PSF structure in the image as well as possible. The result is the image in the upper-right panel of Figure 2; it was used to calculate the NICMOS points in the profile plot panels. Of course, it is not possible to recover the stellar brightness distribution very close to the center. We were conservative and truncated the brightness profile at $r \lesssim 1''$. Uncertainties in the *HST* PSF subtraction do not affect our conclusions. It is important to note that this would not be true at ground-based resolution. The AAT K_s profile does not show the profile kink at $\log r = 0.5$ (see Figure 2 and discussion, below), because the central, fainter part of the profile is filled in by the seeing-convolved Seyfert nucleus.

A comparison of the major-axis, bar, and minor-axis brightness cuts then shows that the “bulge” dominates the brightness distribution at major-axis radii $r < 20''$. Is this a classical bulge or is it a pseudobulge?

The ellipticity profile shows that NGC 4593 contains a pseudobulge, with no sign of a classical bulge component. The apparent ellipticity of the outer disk is $\epsilon \simeq 0.25 \pm 0.05$. Remarkably, the ellipticity of the bulge is also 0.25 ± 0.05 over the whole radius in which we can measure it; i. e., interior to the bar and exterior to the region clobbered by the Seyfert nucleus. Note again that *HST* resolution is important: the extra smoothing caused by the ground-based PSF makes the isophotes as measured with the AAT significantly rounder than those measured with *HST* NICMOS. But the NICMOS data show that the pseudobulge of NGC 4593 is as flat as its disk.

In the absence of PA information, it might be possible that the “bulge” of NGC 4593 is really a nuclear bar. Nuclear bars are common in barred galaxies, and since they have arbitrary position angles with respect to their associated main bars, an elongated “bulge” could be a vertically thick nuclear bar rather than a vertically thin disk. However, the PA is essentially the same at small radii as in the outer disk. For this to be caused by a nuclear bar would require the added accident that the nuclear bar is aligned with the major axis of the galaxy. This is not impossible, but the more likely explanation is that the bulge is nearly circular in its equatorial plane and as flat as the disk.

In either case, the observations imply a pseudobulge. The

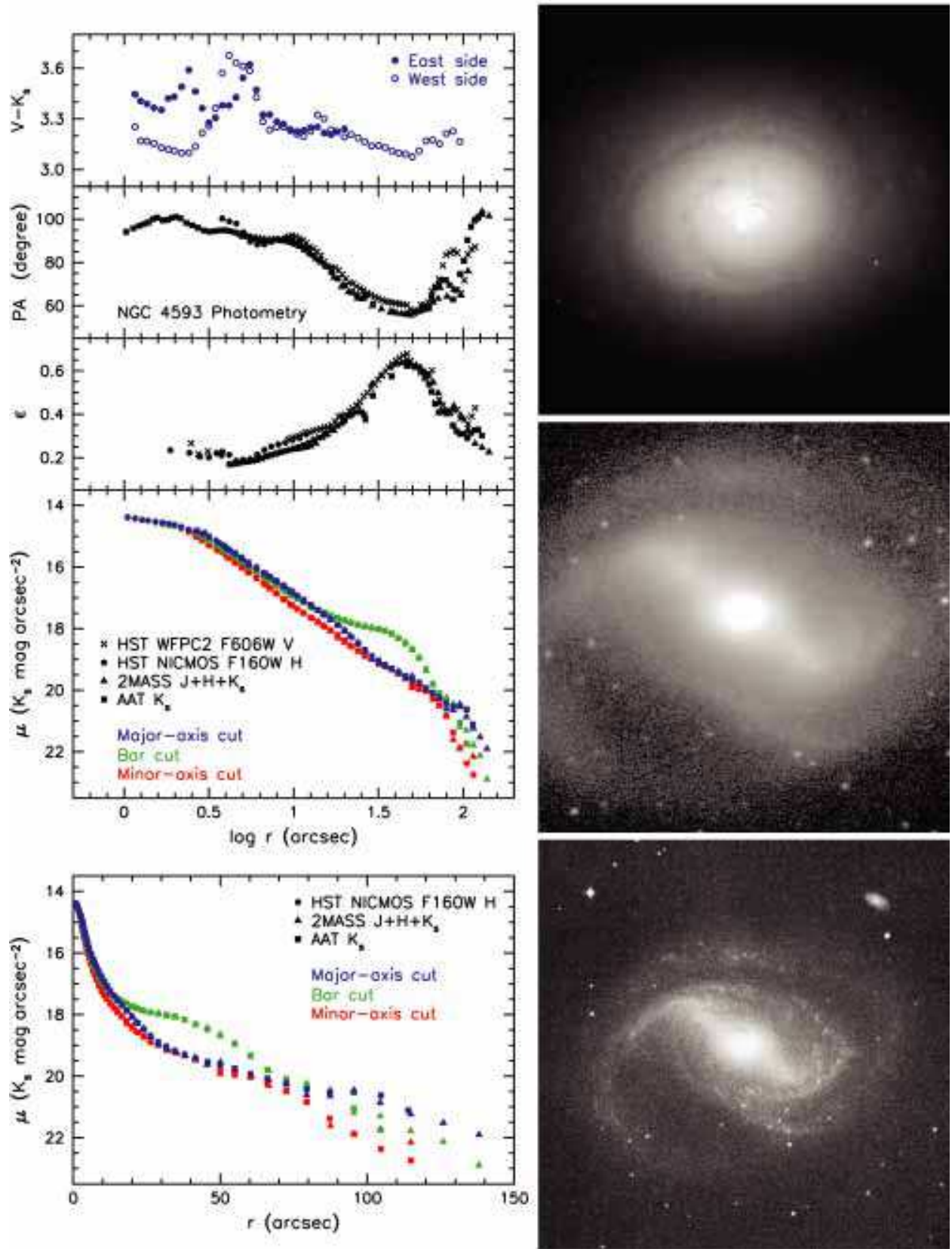


FIG. 2.— NGC 4593 pseudobulge – top image: $18'' \times 18''$ HST NICMOS F160W image from Carollo et al. (2002); middle: $191'' \times 191''$ AAT K_s -band image discussed in §2; the images are shown at different logarithmic intensity stretches. Bottom: $284'' \times 284''$ B -band image from the Carnegie Atlas of Galaxies (Sandage & Bedke 1994). North is up and east is at left in all images. The left panels show surface photometry as a function of \log radius (top) and linear radius (bottom). Brightness profiles are 25° -wide cuts along the major axis (PA = 101°), bar (PA = 57°), and minor axis (PA = 11°) with opposite sides of the galaxy averaged. Isophote ellipticities ϵ and major-axis position angles PA are derived from isophote fits to the images indicated in the key.

cleanest signature of a well developed pseudobulge is that it is very flat. However, since bars are disk phenomena, the

observation of a nuclear bar would also be evidence for a pseudobulge. Both classification criteria are reviewed in KK.

A second feature of the profiles in Figure 2 is consistent with a pseudobulge but does not by itself prove that one is present. The (pseudo)bulge profile has a kink at $\log r \simeq 0.5$ ($r \simeq 3''$). Such features are not seen in classical bulges or ellipticals. The above radius is too large for the kink to be a cuspy core like those in ellipticals (see Lauer et al. 1995; Faber et al. 1997). Pseudobulges are a consequence of more complicated physics than the violent relaxation and dissipation that builds ellipticals. If they grow by star formation in gas that has been transported to the center, exactly how the star formation proceeds and what kind of density profile it produces are controlled by a complicated interplay between star formation (as described by a Schmidt 1959 – Kennicutt 1998a,b law) and the factors – e.g., resonances – that determine where the gas stalls. Nuclear star formation rings seen in many barred and oval galaxies are a hint that the stellar density that “rains out” of the gas distribution may have more complicated radial features than do elliptical galaxies, in which violent relaxation smooths the density in radius. So pseudobulges are likely to have a larger variety of profile shapes than do ellipticals. We see two examples of this variety in the present paper.

4.2. Comparison of V and K_s Images: The Inner Dust Ring as Evidence for Episodic Pseudobulge Growth

Dust is more important in NGC 4593 than in NGC 7690. Therefore we verify in this subsection that dust absorption does not compromise the above conclusions. Examination of the dust features also leads to a new result, namely a hint that the starbursts that contribute most to pseudobulge growth may be episodic.

An inner dust spiral is faintly visible in the top-right panel of Figure 2. Its relationship with the rest of the galaxy is made clear in Figure 3, which shows V -band images that can be compared with K_s images in Figure 2. Figure 3 also shows a $V - K_s$ color image; major-axis cuts through this image are shown in the $V - K_s$ color profile in the top-left panel of Figure 2. We show separately the color profiles east and west of the center; the red “peaks” identify where narrow dust features cross the major axis.

The V -band *HST* PC image (Figure 3) shows a strong dust ring with major-axis radius $\simeq 5''$. It causes the red ring that is the most obvious feature of the $V - K_s$ color image. It is also seen as the red peak in both the east and west color profiles at $\log r \simeq 0.7$ in Figure 2. Interior to the dust ring, the faint dust spiral seen in Figure 2 is, not surprisingly, much more obvious at V band in Figure 3. Its crossings of the major axis are seen in the color profile in Figure 2 as $V - K_s$ maxima at $\log r \simeq 0.6$ on the west side (open circles) and at $\log r \simeq 0.4$ on the east side (filled circles). Fortunately, the dust spiral proves to be very narrow. Over a substantial radius range interior to the dust ring, the colors of the pseudobulge on the west side of the center are closely similar to those in the outer disk. There is no sign of significant reddening or (by inference) absorption at these radii. The minor axis on the south side of the center is similarly free of absorption except in the dust spiral. We used one-sided brightness cuts in these two directions to measure V -band ellipticities at $2''5 \leq r \leq 4''$. These are shown as the crosses in the ϵ profile in Figure 2. The V -band ellipticities, carefully measured to avoid the dust, agree with the K_s values. The same is true at radii outside the dust ring, where dust absorption is small enough

so that V -band isophote fits are possible and both ϵ and PA can be measured. As in the case of NGC 7690, we conclude that the near-infrared measurements, which are much less affected by internal absorption, are reliable. This confirms our conclusions about the flattening of the pseudobulge.

We emphasize again that, except in the very red but narrow dust ring and in the central arcsec, the pseudobulge in NGC 4593 is the same color, $V - K_s \simeq 3.2 \pm 0.1$, as the outer disk at $r \simeq 100''$. Both are about 0.4 mag redder in $V - K_s$ than is NGC 7690. These results again are consistent with Wyse et al. (1997): Bulges and disks both show large ranges in colors, but “bulges are more like their disk[s] than they are like each other.” The red color of NGC 4593 has been noted previously (Santos-Lleó et al. 1995; Shaw et al. 1995). The inner ring and the spiral arms between $r \simeq 30''$ and $80''$ are slightly bluer than the rest of the disk. Inner ring formation is part of the canonical secular evolution picture, and spiral structure is a signature of outward angular momentum transport. But the dust-free parts of the pseudobulge interior to the dust ring are as blue as the outer spiral structure. So the color data are consistent with slow pseudobulge growth.

That growth may be episodic. The $V - K_s$ color image in Figure 3 is instructive. It and the V -band image both show a dust lane on the rotationally leading side of the bar that becomes curved and eventually – near the center – tangent to the nuclear dust ring. Simulations of gas response to a barred potential (see especially Athanassoula 1992; KK provide a review) suggest that such dust lanes occur at shocks where the gas and dust are compressed. Velocity discontinuities across dust lanes observed in HI (e.g., Lindblad et al. 1996; Regan et al. 1997) and HII (Zurita et al. 2004) provide compelling support. If shocks are present, it is inevitable that gas loses energy and falls toward the center. All this is central to the secular evolution picture. Intense starbursts, often in the form of nuclear rings, are commonly associated with the above phenomena (KK provide a detailed review) and are widely interpreted as the result of the gas inflow. This star formation is part of pseudobulge growth. Interestingly, in NGC 4593, we see a nuclear dust ring, not a starburst ring. This suggests that gas is accumulating as a result of bar-driven inflow but that it is not currently starbursting (see also Oliva et al. 1999). Since high gas densities favor high star formation rates (Schmidt 1959; Kennicutt 1998a, b), it is reasonable to assume that the dust and associated gas ring will turn into a star-forming ring some time in the future.

Finally, we return to the one-armed, spiral dust lane that continues inward from the dust ring to the central region that is dominated by the Seyfert nucleus (Malkan et al. 1998; Figure 3 here). Spiral dust lanes interior to star formation rings are also seen in many galaxies (see KK). Elmegreen et al. (1998) suggest that they are a sign that some gas continues to sink toward the center even interior to the radius at which most gas stalls. Additional pseudobulge growth and feeding of the Seyfert nucleus are plausible consequences.

In summary, the V -band *HST* image and the $V - K_s$ color image in Fig. 3 further support our conclusion that bar-driven gas inflow continues to grow a pseudobulge in NGC 4593. They also emphasize a new aspect to the secular evolution picture: the strong starbursts that are seen in many galaxies and that are interpreted as an important part of pseudobulge growth may, at least in some galaxies, be episodic.

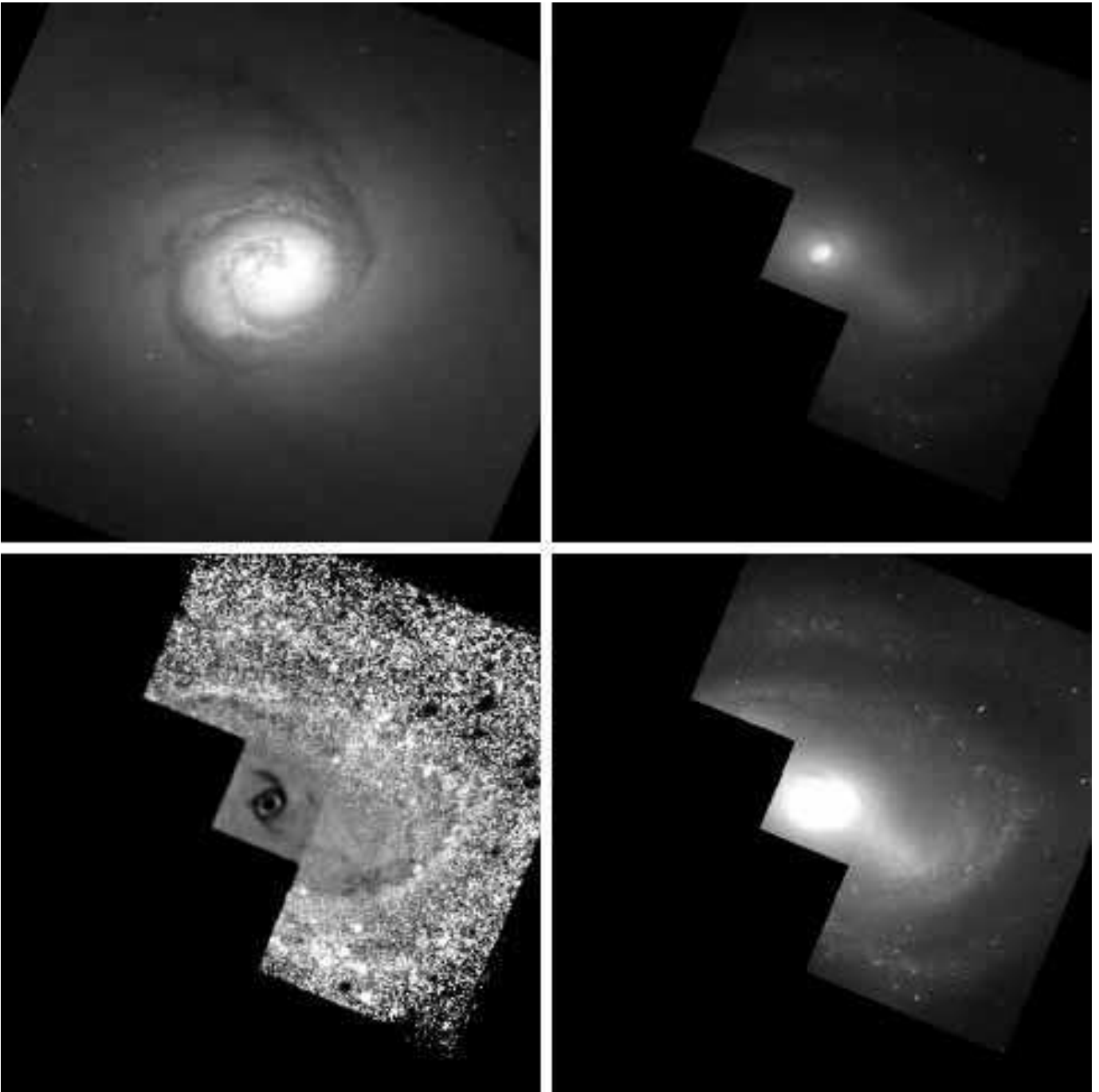


FIG. 3.— NGC 4593 V -band *HST* images (top left, top right, and bottom right) from Malkan et al. (1998) and $V-K_s$ color image (bottom left). The PSF of the Seyfert nucleus was modeled using `Tiny Tim` and has been subtracted. The V -band images are shown at different logarithmic intensity stretches. The intensity stretch of the $V-K_s$ color image is linear in mag arcsec^{-2} ; white corresponds to $V-K_s = 2.9$, and black corresponds to $V-K_s = 4.7$. The top-left panel is $30'' \times 30''$ and can be compared directly with the $18'' \times 18''$ top-right panel in Figure 2. Both show a dust feature starting tangential to the well defined dust ring and spiraling in to the Seyfert nucleus at the center. The other three images are $191'' \times 191''$ and show the same field of view as the middle image panel in Figure 2. They illustrate the relationship between the dust ring with the bar. Almost radial dust lanes in the bar turn into spirals close to the center and become tangential to the dust ring. All of the dust lanes are very red, as shown by the $V-K_s$ image and by the color cuts in the top-left panel of Figure 2.

Kannappan et al. (2004) suggest that accretions of small galaxies are an alternative way to build cold, disk subsystems in galaxies. They find a correlation between blue-centered, star-forming bulges and evidence of tidal encounters with galaxy neighbors. Such processes must happen; embedded counterrotating components provide the clearest examples (e. g., NGC 4826, Braun et al. 1994; Rubin 1994; Walterbos

et al. 1994; Rix et al. 1995; García-Burillo et al. 2003). The observation that so many prominent pseudobulges occur in barred and oval galaxies – that is, ones that contain obvious engines for secular evolution – is one argument that galaxy interactions do not produce most pseudobulges (KK discuss others). These arguments are statistical; they do not much constrain individual galaxies. It is reasonable to ask (as

the referee did): could accreted material account for our observations?

The answer for NGC 7690 is “maybe, but there is no evidence for this”. The answer for NGC 4593 is “probably no”.

First, we need to understand what kind of accretion is possible. Major mergers that happened recently in the history of both galaxies are, we believe, excluded. Tóth & Ostriker (1992) emphasized that disks are fragile; they are easily destroyed by dynamical stirring produced by even a low-mass projectile. Both galaxies have flat components near their centers. Accretion of a high-mass galaxy or one that already has a bulge would destroy such a subsystem and leave behind a big classical bulge that we do not see. This is especially relevant in NGC 4593, which remains flat all the way in to the Seyfert nucleus. What could most safely be accreted is a bulgeless, gas-rich dwarf galaxy; its fluffy stellar distribution would get torn apart by tidal effects at large radii, and its gas could dissipate its way into the central regions.

5.1. NGC 7690

The galaxy is isolated on the Digital Sky Survey. The closest galaxies listed by the NASA/IPAC Extragalactic Database (NED) that have measured recession velocities within 1000 km s^{-1} of that of NGC 7690 are ESO 240-G12 (projected distance = $54.5 = 49$ radii of NGC 7690) and ESO 240-G4 (projected distance = $59.0 = 53$ radii of NGC 7690), where the radius of NGC 7690 at $25 B$ mag arcsec $^{-2}$ is 1.1 (RC3). In an HI survey to look for galaxy pairs (Chengalur et al. 1993), it was not listed as a pair. It has a normal, two-horned, single-dish HI velocity profile with almost no asymmetry (Davies et al. 1989; Chengalur et al. 1993); many isolated, late-type galaxies have more asymmetric velocity profiles. No asymmetry is seen in *The Carnegie Atlas of Galaxies* (Sandage & Bedke 1994), and we see none in our deep AAT images. No interaction appears to be in progress. We cannot exclude a past minor accretion event, but no smoking gun points to one.

5.2. NGC 4593

There are clear signs that NGC 4593 is interacting with PGC 42399. Any such interaction is fast – the velocity difference of 320 km s^{-1} (NED) is large compared with plausible galaxy rotation velocities. This does not favor a strong interaction. Also, NGC 4593 is brighter than PGC 42399 by a factor of 7.7 (NED), so the perturber is not very massive. On the other hand, its projected distance from NGC 4593 is only about two disk radii. The spiral structure of NGC 4593 is slightly distorted toward PGC 42399. Some tidal stretching and possibly some tidal tickling of the wave patterns (spiral arms and bar) in the galaxy are plausible.

Still, the structure of the galaxy is – apart from the above – completely normal (Sandage & Bedke 1994). The galaxy has an inner ring at the end of the bar, as do many other barred galaxies. Such rings are by now reasonably well understood as products of long-term, bar-driven secular evolution. Inner rings are signs that evolution has been going on for a long time. Simulations suggest that the SB(r) phase comes after the SB(s) phase, after outward angular momentum transport has slowed the pattern speed of the bar and after the bar has had time to rearrange disk gas into an inner ring (see KK for a review). This is relevant because simulations also suggest that tidal interactions can trigger bar formation (e.g., Noguchi 1987, 1988; Gerin et al. 1990; Barnes &

Hernquist 1991; Elmegreen et al. 1991, although see also Sellwood 2000). Therefore, although it is tempting to wonder whether the present interaction has something to do with the barred structure of NGC 4593, the mature morphology of the SB(r) structure suggests that the galaxy has been barred and evolving secularly for a long time. The structure of the dust features – a nearly radial dust lane on the leading side of the bar becoming tangent to a nuclear dust ring – are a clear and clean sign of evolution in action (Athanasoula 1992).

Finally, the spiral structure of NGC 4593 is not unusual or suggestive of the influence of the interaction. One arm starts on the inner ring at the end of the bar and the other starts “about 15 degrees downstream” from the end of the bar (Sandage & Bedke 1994). This behavior is similar to that of NGC 2523, another prototypical SB(r) galaxy (Sandage 1961). NGC 2523 is not asymmetric, and it is more isolated than NGC 4594 (the nearest substantial companion, NGC 2523B, is more than 7 NGC 2523 radii away in projection and has a recession velocity 365 km s^{-1} larger than that of NGC 2523; RC3).

Therefore we believe that the present weak and temporary interaction with PGC 42399 is not responsible for the main features of the structure of NGC 4593, including the pseudobulge.

6. CONCLUSION

NGC 7690 (Sab) and NGC 4593 (SBb) provide clean examples of relatively early-type galaxies whose “bulges” are more disk-like than any elliptical galaxy. In particular, elliptical galaxies are never flatter than axial ratio $\simeq 0.4$ (Sandage et al. 1970; Binney & de Vaucouleurs 1981; Tremblay & Merritt 1995), whereas part (NGC 7690) or essentially all (NGC 4593) of the bulges of the present galaxies are as flat as their outer disks. We conclude that both galaxies contain pseudobulges – that is, high-density, central components that were made out of disk gas by secular evolution. In NGC 7690, blue colors imply that star formation and hence pseudobulge growth are still in progress. In NGC 4593, gas appears currently to be accumulating in a ring that plausibly will form stars in the future. Our results are examples of the general conclusion (see KK for a review) that secular dynamical evolution occurs naturally and often in disk galaxies, whether (NGC 4593) or not (NGC 7690) an engine for the evolution is readily recognized.

To further investigate secular evolution, a desirable next step would be to quantify bar strengths by measuring bar torques, the ratio of the bar-induced, tangential force to the mean radial force as a function of radius (Buta & Block 2001; Laurikainen & Salo 2002; Block et al. 2001, 2004; Laurikainen et al. 2004). This ratio can be as high as 0.6 in strong bars, emphasizing how efficient bars can be in redistributing angular momentum. It would particularly be worthwhile to look for correlations between maximum bar torques and quantifiable consequences of secular evolution (e.g., ring-to-disk and pseudobulge-to-disk mass ratios) in a statistically representative sample of galaxies.

JK is sincerely grateful to Mrs. M. Keeton and the Board of Trustees of the Anglo American Chairman’s Fund for the financial support that made possible his visit to South Africa during which this paper was written. He also thanks the Cosmic Dust Laboratory and the School of Computational and Applied Mathematics of the University of the Witwatersrand for their hospitality. JHK acknowledges

support from the Leverhulme Trust in the form of a Leverhulme Research Fellowship. We thank the referee for a careful reading that led to substantial improvements to this paper. JHK and EA wish to thank the staff of the AAT, and in particular Dr. Stuart Ryder, for their excellent support during his observing run with IRIS2. The authors are grateful to Ron Buta, to Bruce and Debra Elmegreen, and to Ivanio Puerari for making data from their programs with DLB and JHK available for the present

work. We also thank Roberto Saglia for his version of the Bender photometry pipeline. This research has made use of the NASA/IPAC Extragalactic Database (NED), which is operated by the Jet Propulsion Laboratory, California Institute of Technology, under contract with NASA. This research also used the HyperLeda electronic database at <http://www-obs.univ-lyon1.fr/hypercat> and the image display tool SAOImage DS9 developed by the Smithsonian Astrophysical Observatory.

REFERENCES

- Athanassoula, E. 1992, *MNRAS*, 259, 345
- Banse, K., Ponz, D., Ounnas, C., Grosbøl, P., & Warmels, R. 1988, in *Instrumentation for Ground-Based Optical Astronomy: Present and Future*, ed. L. B. Robinson (New York: Springer), 431
- Barnes, J. E., & Hernquist, L. E. 1991, *ApJ*, 370, L65
- Bender, R., Döbereiner, S., & Möllenhoff, C. 1988, *A&AS*, 74, 385
- Bender, R., & Möllenhoff, C. 1987, *A&A*, 177, 71
- Bertin, E., & Arnouts, S. 1996, *A&AS*, 117, 393
- Binney, J., & de Vaucouleurs, G. 1981, *MNRAS*, 194, 679
- Block, D. L., Buta, R., Knapen, J. H., Elmegreen, D. M., Elmegreen, B. G., & Puerari, I. 2004, *AJ*, 128, 183
- Block, D. L., Puerari, I., Knapen, J. H., Elmegreen, B. G., Buta, R., Stedman, S., & Elmegreen, D. M. 2001, *A&A*, 375, 761
- Braun, R., Walterbos, R. A. M., Kennicutt, R. C., & Tacconi, L. J. 1994, *ApJ*, 420, 558
- Buta, R., & Block, D. L. 2001, *ApJ*, 550, 243
- Buta, R., & Combes, F. 1996, *Fund. Cosmic Phys.*, 17, 95
- Carollo, C. M., Ferguson, H. C., & Wyse, R. F. G., ed. 1999, *The Formation of Galactic Bulges* (Cambridge: Cambridge University Press)
- Carollo, C. M., Stiavelli, M., & Mack, J. 1998, *AJ*, 116, 68
- Carollo, C. M., Stiavelli, M., Seigar, M., de Zeeuw, P. T., & Dejonghe, H. 2002, *AJ*, 123, 159
- Cawson, M. G. M. 1983, Ph. D. Thesis, University of Cambridge
- Chengalur, J. N., Salpeter, E. E., & Terzian, Y. 1993, *ApJ*, 419, 30
- Courteau, S. 1996, in *New Extragalactic Perspectives in the New South Africa*, ed. D. L. Block & J. M. Greenberg (Dordrecht: Kluwer), 255
- Courteau, S., de Jong, R. S., & Broeils, A. H. 1996, *ApJ*, 457, L73
- Cox, A. N., ed. 2000, *Allen's Astrophysical Quantities*, Fourth Edition (New York: Springer)
- Davies, R. D., Staveley-Smith, L., & Murray, J. D. 1989, *MNRAS*, 236, 171
- Davis, L. E., Cawson, M., Davies, R. L., & Illingworth, G. 1985, *AJ*, 90, 169
- de Vaucouleurs, G., de Vaucouleurs, A., Corwin, H. G., Buta, R. J., Paturel, G., & Fouqué, P. 1991, *Third Reference Catalogue of Bright Galaxies* (New York: Springer) (RC3)
- Elmegreen, B. G., et al. 1998, *ApJ*, 503, L119
- Elmegreen, D. M., Sundin, M., Elmegreen, B., & Sundelius, B. 1991, *A&A*, 244, 52
- Erwin, P. 2005, *MNRAS*, 364, 283
- Faber, S. M., et al. 1997, *AJ*, 114, 1771
- Freeman, K. C. 1975, in *IAU Symposium 69, Dynamics of Stellar Systems*, ed. A. Hayli (Dordrecht: Reidel), 367
- Gadotti, D. A., & dos Anjos, S. 2001, *AJ*, 122, 1298
- García-Burillo, S., et al. 2003, *A&A*, 407, 485
- Gerin, M., Combes, F., & Athanassoula, E. 1990, *A&A*, 230, 37
- Holtzman, J. A., Burrows, C. J., Casertano, S., Hester, J. J., Trauger, J. T., Watson, A. M., & Worthey, G. 1995, *PASP*, 107, 1065
- Jarrett, T. H., Chester, T., Cutri, R., Schneider, S. E., & Huchra, J. P. 2003, *AJ*, 125, 525
- Kannappan, S. J., Jansen, R. A., & Barton, E. J. 2004, *AJ*, 127, 1371
- Kennicutt, R. C. 1998a, *ApJ*, 498, 541
- Kennicutt, R. C. 1998b, *ARA&A*, 36, 189
- Knapen, J. H., de Jong, R. S., Stedman, S., & Bramich, D. M. 2003, *MNRAS*, 344, 527
- Kormendy, J. 1979, *ApJ*, 227, 714
- Kormendy, J. 1981, in *The Structure and Evolution of Normal Galaxies*, ed. S. M. Fall & D. Lynden-Bell (Cambridge: Cambridge Univ. Press), 85
- Kormendy, J. 1984, *ApJ*, 286, 116
- Kormendy, J. 1993, in *IAU Symposium 153, Galactic Bulges*, ed. H. Dejonghe & H. J. Habing (Dordrecht: Kluwer), 209
- Kormendy, J., & Cornell, M. E. 2004, in *Penetrating Bars Through Masks of Cosmic Dust: The Hubble Tuning Fork Strikes a New Note*, ed. D. L. Block, I. Puerari, K. C. Freeman, R. Groess, & E. K. Block (Dordrecht: Kluwer), 261
- Kormendy, J., & Fisher, D. B. 2005, in *The Ninth Texas-Mexico Conference on Astrophysics*, *RevMexA&A*, (Serie de Conferencias), 23, 101
- Kormendy, J., & Kennicutt, R. C. 2004, *ARA&A*, 42, 603
- Krist, J., & Hook, R. 2004, *The Tiny Tim User's Guide* (Baltimore: Space Telescope Science Institute)
- Lauer, T. R., et al. 1995, *AJ*, 110, 2622
- Lauer, T. R., Stover, R. J., & Terndrup, D. 1983, *The VISTA Users Guide*, Lick Observatory Technical Report 34
- Laurikainen, E., & Salo, H. 2002, *MNRAS*, 337, 1118
- Laurikainen, E., Salo, H., Buta, R., & Vasylyev, S. 2004, *MNRAS*, 355, 1251
- Lewis, D. W., MacAlpine, G. M., & Koski, A. T. 1978, *BAAS*, 10, 388
- Lindblad, P. A. B., Lindblad, P. O., & Athanassoula, E. 1996, *A&A*, 313, 65
- Lynden-Bell, D., & Kalnajs, A. J. 1972, *MNRAS*, 157, 1
- Lynden-Bell, D., & Pringle, J. E. 1974, *MNRAS*, 168, 603
- Malkan, M. A., Gorjian, V., & Tam, R. 1998, *ApJS*, 117, 25
- MacAlpine, G. M., Williams, G. A., & Lewis, D. W. 1979, *PASP*, 91, 746
- McAlary, C. W., McLaren, R. A., McGonegal, R. J., & Maza, J. 1983, *ApJS*, 52, 341
- Noguchi, M. 1987, *MNRAS*, 228, 635
- Noguchi, M. 1988, *A&A*, 203, 259
- Oliva, E., Origlia, L., Maiolino, R., & Moorwood, A. F. M. 1999, *A&A*, 350, 9
- Pelletier, R. F., & Balcells, M. 1996, *AJ*, 111, 2238
- Prugniel, Ph., & Héraudeau, Ph. 1998, *A&AS*, 128, 299
- Renzini, A. 1999, in *The Formation of Galactic Bulges*, ed. C. M. Carollo, H. C. Ferguson, & R. F. G. Wyse (Cambridge: Cambridge University Press), 9
- Regan, M. W., Vogel, S. N., & Teuben, P. J. 1997, *ApJ*, 482, L143
- Rix, H.-W. R., Kennicutt, R. C., Braun, R., & Walterbos, R. A. M. 1995, *ApJ*, 438, 155
- Rubin, V. C. 1994, *AJ*, 107, 173
- Sandage, A. 1961, *The Hubble Atlas of Galaxies*, (Washington: Carnegie Institution of Washington)
- Sandage, A., & Bedke, J. 1994, *The Carnegie Atlas of Galaxies* (Washington: Carnegie Institution of Washington)
- Sandage, A., Freeman, K. C., & Stokes, N. R. 1970, *ApJ*, 160, 831
- Santos-Lleó, M., Clavel, J., Barr, P., Glass, I. S., Pelat, D., Peterson, B. M., & Reichert, G. 1995, *MNRAS*, 274, 1
- Schlegel, D. J., Finkbeiner, D. P., & Davis, M. 1998, *ApJ*, 500, 525
- Schmidt, M. 1959, *ApJ*, 129, 243
- Schweizer, F. 1990, in *Dynamics and Interactions of Galaxies*, ed. R. Wielen (New York: Springer-Verlag), 60
- Sellwood, J. A. 2000, in *Dynamics of Galaxies: From the Early Universe to the Present*, ed. F. Combes, G. A. Mamon, & V. Charmandaris (San Francisco: ASP), 3
- Sellwood, J. A., & Wilkinson, A. 1993, *Rep. Prog. Phys.*, 56, 173
- Sérsic, J. L. 1968, *Atlas de Galaxias Australes* (Cordoba: Observatorio Astronomico, Universidad de Cordoba)
- Shaw, M., Axon, D., Probst, R., & Gatley, I. 1995, *MNRAS*, 274, 369
- Simien, F., & de Vaucouleurs, G. 1986, *ApJ*, 302, 564
- Spergel, D. N., et al. 2003, *ApJS*, 148, 175
- Steinmetz, M., & Navarro, J. F. 2002, *NewA*, 7, 155
- Steinmetz, M., & Navarro, J. F. 2003, *NewA*, 8, 557
- Stover, R. J. 1988, in *Instrumentation for Ground-Based Optical Astronomy: Present and Future*, ed. L. B. Robinson (New York: Springer), 443
- Tinney, C. G., et al. 2004, *Proc. SPIE*, 5492, 998
- Tody, D. 1986, *Proc. SPIE*, 627, 733
- Toomre, A.: 1977, in *The Evolution of Galaxies and Stellar Populations*, ed. B. M. Tinsley & R. B. Larson (New Haven: Yale University Observatory), 401
- Tóth, G., & Ostriker, J. P. 1992, *ApJ*, 389, 5
- Tremaine, S. 1989, in *Dynamics of Astrophysical Discs*, ed. J. A. Sellwood (Cambridge: Cambridge Univ. Press), 231
- Tremblay, B., & Merritt, D. 1995, *AJ*, 110, 1039
- Tully, R. B. 1988, *Nearby Galaxies Catalog* (Cambridge: Cambridge University Press)
- van Dokkum, P. G. 2001, *PASP*, 113, 1420
- Walterbos, R. A. M., Braun, R., & Kennicutt, R. C. 1994, *AJ*, 107, 184
- Wegner, G. 1979, *Ap&SS*, 60, 15
- Wyse, R. F. G., Gilmore, G., & Franx, M. 1997, *ARA&A*, 35, 637
- Zurita, A., Relaño, M., Beckman, J. E., & Knapen, J. H. 2004, *A&A*, 413, 73